

# We are IntechOpen, the world's leading publisher of Open Access books Built by scientists, for scientists

5,000

Open access books available

125,000

International authors and editors

140M

Downloads

Our authors are among the

154

Countries delivered to

TOP 1%

most cited scientists

12.2%

Contributors from top 500 universities



WEB OF SCIENCE™

Selection of our books indexed in the Book Citation Index  
in Web of Science™ Core Collection (BKCI)

Interested in publishing with us?  
Contact [book.department@intechopen.com](mailto:book.department@intechopen.com)

Numbers displayed above are based on latest data collected.  
For more information visit [www.intechopen.com](http://www.intechopen.com)



# Recovery of Photovoltaic Module Heat Using Thermoelectric Effect

*Felix A. Farret and Emanuel A. Vieira*

## Abstract

The growing demand for renewable energy sources, in particular for solar technologies, requires more detailed studies to increase power and efficiency. Among them, thermoelectric energy conversion is a well-known technology used for decades including solar thermal generators (STEG), radioisotope thermoelectric generators (RTG), automotive thermoelectric generators (ATG) and thermoelectric generators (TEG). This chapter aims to demonstrate that the thermoelectric effect (Seebeck effect) can be used to harness the thermal energy retained in photovoltaic panels to increase their overall efficiency with its direct conversion into electrical energy and vice versa. It is also observed that solar radiation can be converted directly into electric energy, as in photovoltaic modules, or yet can be converted directly into electricity, as in thermoelectric modules. It is emphasised that although the energy conversion by thermoelectric effect still has low electrical efficiency, this source is characterised by a high degree of reliability, low maintenance, appreciable durability and absence of moving parts, and it allows generating electric energy through recovery of the thermal energy from several industrial processes. At the end of this chapter is presented a case study related to the thermal energy absorbed by a polycrystalline photovoltaic module to illustrate their increased efficiency and power in thermoelectric-photovoltaic cogeneration.

**Keywords:** photovoltaic-thermoelectric cogeneration, thermal energy, thermoelectric effect, renewable energy sources, solar energy

## 1. Introduction

In this chapter, the thermoelectric effect is used to exploit the thermal energy accumulated in the operation of photovoltaic panels, reversing it into electric energy. For this, a brief presentation of the thermoelectric effect is made to obtain an equivalent circuit of a thermoelectric module and its associations (series and parallel).

Traditionally, the term thermoelectric effect or thermoelectricity involves three effects that can be identified separately: the Seebeck effect, the Peltier effect and the Thomson effect. **Figure 1** illustrates these three thermoelectric effects.

From the discovery of Alessandro Volta related to the production of electricity by the mere contact between different metals, the researches on thermoelectricity took

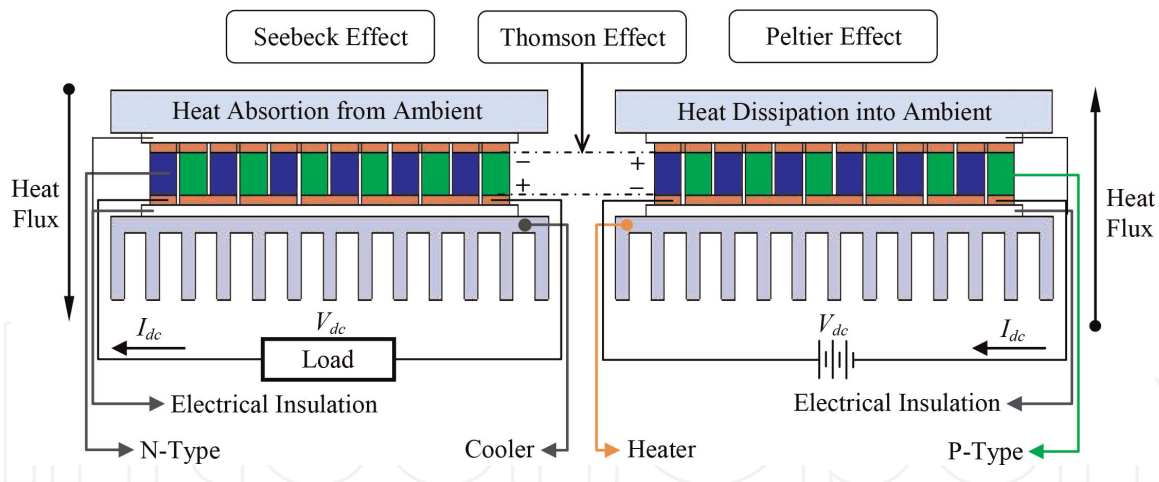


**Figure 1.**  
Thermoelectric effect.

impulse and began looking for the origin of the thermoelectric effects [1]. These effects can be reunited as follows:

- Seebeck effect (1822) explaining that an emf is generated by a pair of different conductors whose ends are not at the same temperature with respect to their junction.
- Peltier effect (1834) which refers to the release or absorption of heat at the junction of two different materials when an electric current flows through from one conductor to the other.
- Joule effect (1840) that relates the production of heat at a given time whenever the material is carrying electric charges.
- Thomson effect (1856) refers to the production or absorption of heat when an electric current passes through a circuit made of a single material and under a temperature difference across its length.

The material properties listed above are used to explain how the thermoelectric effect is able to produce a direct conversion of a temperature difference into an electrical voltage and vice versa. On the left side of **Figure 1**, the thermal Seebeck effect appears as a temperature gradient on the faces of a thermoelectric module coupled to a pair of semiconductors, whereby an electric current flows through the N-P direction of the junction. The Peltier effect represented on the right side of **Figure 1** consists of the production of a temperature gradient across the junction between two conductors (or semiconductors) of different materials in a closed loop when subjected to an electric voltage. On the other hand, thermoelectric generators can act as heat engines, being less bulky and having no moving parts [2].

In principle, the association of the Peltier-Seebeck and Thomson effects may be thermodynamically reversible, whereas the Joule effect is not reversible. This nonreversibility of the Joule effect causes many authors to consider the existence of only two thermoelectric effects.

## 2. Thermoelectric materials

The application of semiconductor materials in the construction of thermocouples in some special cases has contributed significantly for electricity generation,

refrigeration and heating, as well as being of interest to theoretical physics based on the modern science of semiconductors. The energy applications of these thermoelements are mainly in thermoelectric coolers, industrial and domestic heating devices, thermoelectrically generated sound, ultrasonic generators, vacuum thermoelements, space applications in satellite power, marine applications in buoys and headlights, as well as in medicine applications of cardiac pacemaker feeding.

For the sake of completeness, the principle of direct conversion of thermal energy into electricity is also widely used today in temperature measurements by means of thermocouples or thermo-junctions based on metals or metal alloys. In this particular, **Table 1** shows the Seebeck coefficient for some metal alloys and semiconductors used to make thermoelectric modules on a commercial scale.

The economical and practical applications of thermoelectric materials depend on the characteristics of the available thermoelements, their efficiency, temperatures involved in the operation, stability of operation and costs involving raw materials in the final preparation. As a rule, it should be noted that the thermal cycle of a thermoelectric generation differs from others because it consists essentially of a solid-state phenomenon where the thermal energy is converted directly into electric energy. This direct conversion has made possible the construction of simple devices such as transducers or power sources, which have practically no maintenance and no moving parts, which makes them highly interesting in exact sciences.

The thermoelectric materials can be made of conductors, semiconductors and insulators. In a more careful classification, it is necessary to take into account the microscopic characteristics referring to the electron behaviour in the valence layer of the material by action of an electric field [3]. A thermoelectric material with high electrical conductivity, high Seebeck coefficient and low thermal conductivity can be considered a good thermoelectric material [4].

It should be said at this stage that the efficiency of a thermoelectric device depends both on the operating temperature of the materials and on the characteristics of these materials, which can be expressed by the figure of merit given in Eq. (1).

Semiconductor	Seebeck coefficient ( $\mu\text{V}/^\circ\text{C}$ )
$\text{Bi}_2\text{Te}_3$ (P-type)	-230
$\text{Bi}_{2x}\text{Sb}_x\text{Te}_3$ (P-type)	300
$\text{Sb}_2\text{Te}_3$ (P-type)	185
PbTe	-180
$\text{Pb}_3\text{Ge}_{39}\text{Se}_{58}$	1670
$\text{Pb}_6\text{Ge}_{36}\text{Se}_{58}$	1410
$\text{Pb}_9\text{Ge}_{33}\text{Se}_{58}$	-1360
$\text{Pb}_{13}\text{Ge}_{29}\text{Se}_{58}$	-1710
$\text{Pb}_{15}\text{Ge}_{37}\text{Se}_{58}$	-1990
$\text{SnBi}_4\text{Te}_7$	120
$\text{SnBi}_3\text{Sb}_1\text{Te}_7$	151
$\text{SnBi}_{2.5}\text{Sb}_{1.5}\text{Te}_7$	110
$\text{SnBi}_2\text{Sb}_2\text{Te}_7$	90
$\text{PbBi}_4\text{Te}_7$	-53

**Table 1.**  
 Seebeck coefficients for metal alloys and semiconductors.

$$Z = \frac{\alpha^2}{\sigma\kappa} \quad (1)$$

where:

$\alpha$  is the Seebeck coefficient.

$\sigma$  is the electric conductivity.

$\kappa$  is the thermal conductivity.

$Z$  is the figure of merit.

Eq. (2) relates the figure of merit to temperature. However, the figure of merit does not have a constant behaviour as the temperature varies [1], but it can also be expressed in a dimensionless form  $Z\bar{T}$  [4]:

$$Z\bar{T} = \left(\frac{\alpha^2}{\sigma\kappa}\right)\bar{T} \quad (2)$$

where:

$\bar{T}$  is the average temperature between the faces (hot and cold).

$Z\bar{T}$  is the figure of merit dependent on temperature.

### 3. Thermoelectric module

A “modern” thermoelectric converter essentially consists of a series of thermoelectric semiconductors of N-type and P-type materials alternately connected. It is noticeable that these semiconductor elements are electrically connected in series and thermally in parallel by a series of metal contacts placed at each two ceramic plates (**Figure 2a**).

A typical thermoelectric device consists of two ceramic substrates (alumina) (**Figure 2a**), which serves both as base and electrical insulation, for thermoelements (e.g. bismuth telluride) electrically connected in series and thermally in parallel as in the case of ceramics [1]:

$$T_{\max} = 0.5Z \cdot T \quad (3)$$

Conventional thermoelectric devices have various specifications according to the type of application. The dimensions commonly range from 3 to 5 mm in thickness and from 56 to 60 mm in lateral length. The faces exposed to the outside have a square geometry. The maximum rate of heat pumping varies from 1 to 125 W [5].

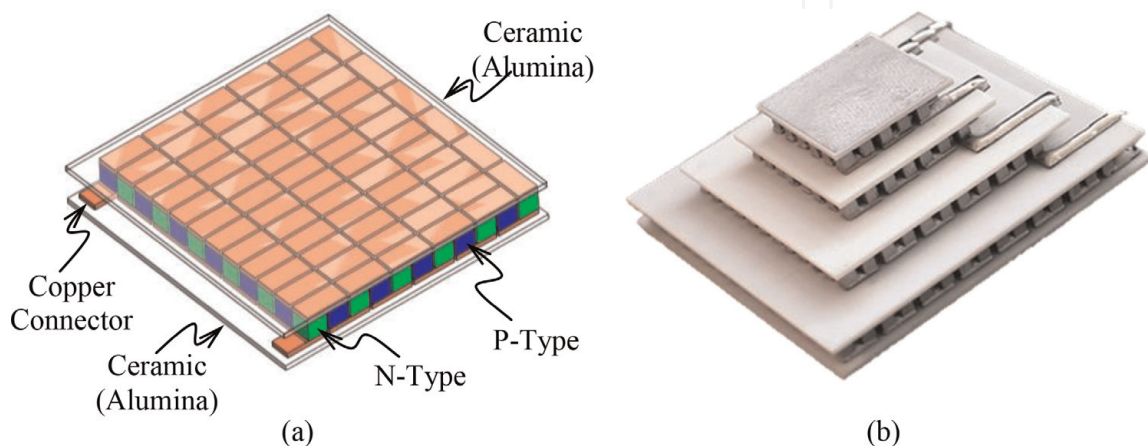


**Figure 2.** Thermoelectric module: (a) single TEG and (b) multistage TEG.

The maximum temperature difference between the hot and cold sides can reach 70° C. Typical thermoelectric modules contain from 3 to 127 thermocouples.

There are multistage (cascade) thermoelectric devices designed to meet the requirements of large temperature differentials ( $\Delta T$  can reach 130°C). The lowest achievable temperature is  $< -100^\circ\text{C}$  for multistage devices [5].

There are thermoelectric modules made up of several layers known as multistage thermoelectric modules (see **Figure 2b**). The maximum temperature difference obtained between the interfaces of each layer in a multistage thermoelectric module is given by Eq. (3).

#### 4. Equivalent circuit of thermoelectric modules

Section 1 explained how the Seebeck effect could generate an electrical voltage from a temperature difference between the junction of two distinct semiconductor materials and the ends of them. Eq. (4) states that the higher the temperature differences between the thermoelectric junctions, the greater the electric potential generated [6]:

$$V = N_j \int_{T_1}^{T_2} [\alpha_2(T) - \alpha_1(T)] dt \quad (4)$$

where:

$N_j$  is the number of junctions for identical thermoelectric pairs.

$T_1$  and  $T_2$  are the temperatures at the extremes of the material pair.

$\alpha_1$  and  $\alpha_2$  are the Seebeck coefficients of the semiconductor materials.

The equivalent electrical circuit of a thermoelectric module can be seen in **Figure 3a**, where the output voltage  $V_i$  across the terminals of a no-load module is given by Eq. (5). As this circuit is not connected to any load, it does not circulate electrical current through it:

$$V_i = \alpha \Delta T \quad (5)$$

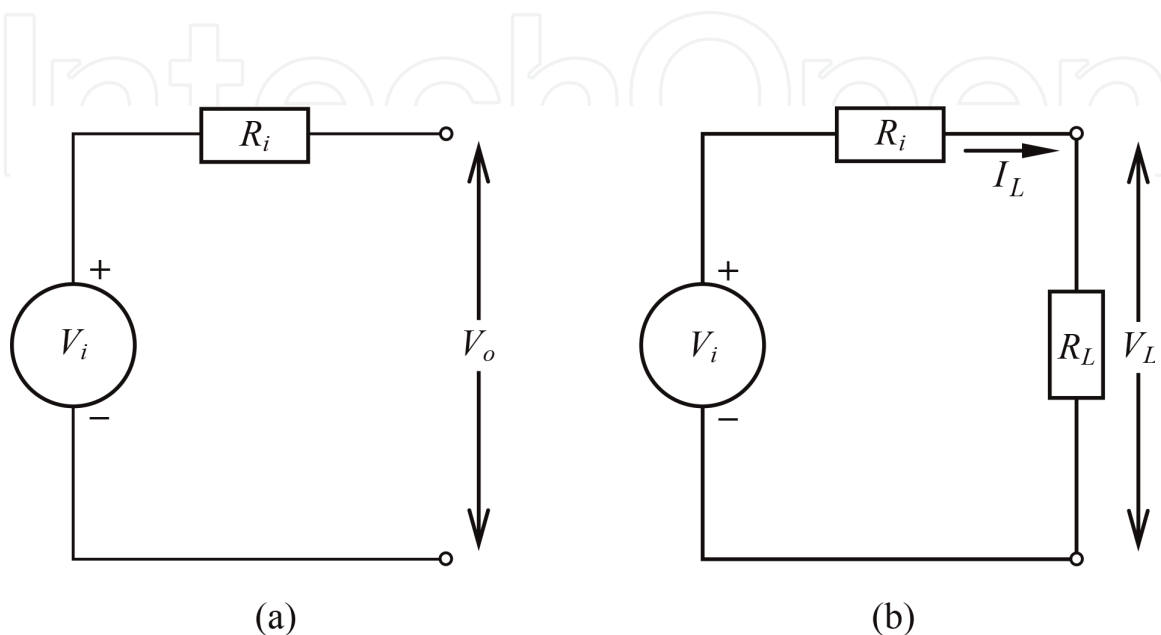


**Figure 3.**  
 Equivalent electric circuit: (a) open circuit and (b) circuit with load.



where:

$V_i$  is the input source voltage.

$\alpha$  is the absolute coefficient of Seebeck.

$\Delta T$  is the temperature difference between faces of the thermoelectric module.

When a load  $R_L$  is connected across the circuit terminals of **Figure 3b**, a current  $I_L$  will flow through it according Eq. (6):

$$I_L = \frac{V_i}{R_i + R_L} \quad (6)$$

It is shown in **Figure 3b** that the load voltage  $V_L$  can be defined as the total voltage generated minus the internal voltage drops in the module, as in Eq. (7) [7]:

$$V_L = V_i - I_L R_i \quad (7)$$

Eq. (7) can then be rewritten in terms of temperature difference and the Seebeck coefficient by replacing  $I_L$  given by Eq. (6) and  $V_i$  given by Eq. (5). The load voltage  $V_L$  can be rewritten as a function of the temperature and the Seebeck coefficient as in Eq. (8):

$$V_L = \alpha \Delta T - \frac{\alpha \Delta T}{R_i + R_L} R_i \quad (8)$$

The power generated by a thermoelectric module is a function of the generated voltage as given by Eq. (9):

$$P_L = \frac{V_i^2 R_L}{(R_i + R_L)^2} \quad (9)$$

The power dissipated in the load can also be expressed as a function of the temperature difference across the faces of the thermoelectric module, according to Eq. (10):

$$P_L = \frac{(\alpha^2 \Delta T^2) R_L}{(R_i + R_L)^2} \quad (10)$$

Mathematically, the maximum power in the load  $P_{L, \max}$  is obtained by deriving the expression of electric power in relation to  $R_L$  and equalling to zero according to Eq. (11):

$$\frac{V_i^2 (R_i + R_L) - 2 R_L V_i^2}{(R_i + R_L)^2} = 0 \quad (11)$$

Based on the identity of Eq. (11), it is concluded that  $R_L = R_i$ , both nonzero resistors. The internal resistance  $R_i$  of each thermoelectric module is obtained by the algebraic sum of the internal thermal resistances of the metallic material of the junction with the sum of resistances of the N-P junctions and with the thermal resistance of the physical contacts [8].

By making  $R_i = R_L = R_{\max, \text{pot}}$  and replacing everything in Eq. (10), the maximum power is given as a function of temperature by Eq. (12) [9]:

$$P_{L, \max} = \frac{\alpha^2 \Delta T^2}{4 R_{\max, \text{pot}}} \quad (12)$$

It should be noted that the performance of a thermoelectric module can be characterised by the Seebeck coefficient, the internal resistance and the thermal

conductance [7]. The thermal conductance of the thermoelectric module is given as a function of the thermal conductance of each P-N junction. As the P-N elements have equal volumes, the thermal conductance will be the same for both semiconductors, and it is expressed by Eq. (13) [7]:

$$K = 2 \frac{kA_j}{l} \quad (13)$$

where:

$A_j$  is the area of each thermoelectric junction.

$\kappa$  is the thermal conductivity.

$l$  is the thermoelectric module length.

The heat absorbed  $\dot{Q}_h$  and the heat removed  $\dot{Q}_c$  are expressed by Eqs. (14) and (15) [7]:

$$\dot{Q}_h = \alpha I_L T_h + K(T_h - T_c) - \frac{1}{2} I_L^2 R_i \quad (14)$$

$$\dot{Q}_c = \alpha I_L T_c + K(T_h - T_c) - \frac{1}{2} I_L^2 R_i \quad (15)$$

where:

$T_h$  is the temperature of the hot face of the thermoelectric pair.

$T_c$  is the temperature of the cold face of the thermoelectric.

$\alpha I_L T_h$  is the heat rate of the thermoelectric module.

$\alpha I_L T_c$  is the heat rate of the thermoelectric module.

$\frac{1}{2} I_L^2 R_i$  is the power dissipated.

$K(T_h - T_c)$  is the heat pumping between two thermal reservoirs.

The efficiency of the thermoelectric module can be obtained from the ratio of the electric output power  $P_L$  and the heat received in the thermoelectric module according to Eq. (16):

$$\eta_{TEG} = \frac{P_L}{\dot{Q}_q} \quad (16)$$

According to [10], the heat transferred through the module determines the thermoelectric efficiency. Therefore, the thickness of the module is the parameter that most affects the efficiency which is expressed as in Eq. (17):

$$\eta_{TEG} = \frac{I_L^2 R_L w_t}{\kappa A_{TEG} \Delta T} \quad (17)$$

where:

$w_t$  is the thickness of the thermoelectric module.

$A_{TEG}$  is the face area of the thermoelectric module.

## 5. Association of thermoelectric modules

The arrangement of connections between thermoelectric modules resembles that of the photovoltaic modules, which can be arranged in series or in parallel. If the objective is to increase the electrical voltage across the thermoelectric modules, the series connection must be used. If the aim is to increase the current through the modules, they must be connected in parallel. A third option is a mixed



series-parallel arrangement that provides an increase in power either by the increase in voltage or current or both. In this way, the load current generated by the association of the thermoelectric modules is represented by Eq. (18) [10]:

$$I_L = \frac{N_s \alpha \Delta T}{\frac{N_i R_i}{N_p} + R_L} \quad (18)$$

where:

$N_s$  and  $N_p$  are, respectively, the number thermoelectric modules in series and parallel.

The voltage generated across the load by an arrangement of thermoelectric modules is given by Eq. (19) [10]:

$$V_L = R_L \left( \frac{N_s \alpha \Delta T}{\frac{N_i R_i}{N_p} + R_L} \right) \quad (19)$$

The maximum thermoelectric power occurs when the internal resistance  $R_i$  is equal to the load resistance  $R_L$ , and it is given by Eq. (20) [10]:

$$P_{L, \max} = \frac{N_T [\alpha (T_h - T_c)]^2}{4 R_i} \quad (20)$$

where:

$N_T$  is the total number of modules.

With Eq. (21) it is possible to determine the heat input in the thermoelectric generator in watts [10]:

$$\dot{Q}_w = N_T \left[ \frac{\alpha T_h I_L}{N_T} - 0.5 R_i \left( \frac{I_L}{N_p} \right)^2 + k(T_h - T_c) \right] \quad (21)$$

where:

$N_T$  is the total number of thermoelectric modules.

The efficiency of the thermoelectric generator is given by Eq. (22), which relates the maximum power generated with the array of modules and the amount of heat that had been absorbed by the array [10]:

$$\eta_{TEG} = \frac{P_{L, \max}}{\dot{Q}_w} \quad (22)$$

## 6. Layer temperatures in the photovoltaic modules

The determination of the temperature in a photovoltaic module is of great importance for thermoelectric generation. For this, a Ross model was developed to simplify the determination of temperature in a photovoltaic cell located between the layers of the photovoltaic modules caused by the ambient temperature and solar radiation as shown in **Figure 4**.

Ross determined the temperature coefficients for photovoltaic cells according to the residential installation form (**Table 2**) [11, 12].

From the Ross observation, the temperature of the photovoltaic cell can be determined with Eq. (23) [11, 12]:

$$T_{Cell} = T_{amb}K_S G_i \quad (23)$$

where:

$T_{amb}$  is the ambient temperature.

$K_S$  is the coefficient of Ross.

$G_i$  is solar radiation.

The mechanism of heat transfer between layers that cause the temperature difference between the photovoltaic cell and the polyvinyl fluoride layer, which commercial trade mark is Tedlar®, occurs by conduction and can be expressed by Eq. (24) [13]:

$$T_{Cell} - T_{Tedlar} = \frac{\dot{Q}}{\sum R_{thermal}} \quad (24)$$

where:

$\sum R_{thermal}$  is the sum of the thermal resistances of the photovoltaic cell.

$\dot{Q}$  is the useful energy of solar radiation.

$T_{Tedlar}$  is the temperature of Tedlar®.

$T_{cell}$  is the temperature of the photovoltaic cell.

**Table 3** lists the thickness of the photovoltaic module layers with the thermal conductivities of each constituent. The thermal resistance between the Glass-Tedlar® layers is determined then by Eq. (25) [13]:

$$\sum R_{thermal} = \frac{d_{Glass}}{k_{Glass}} + \frac{d_{EVA}}{k_{EVA}} + \frac{d_{Tedlar}}{k_{Tedlar}} \quad (25)$$

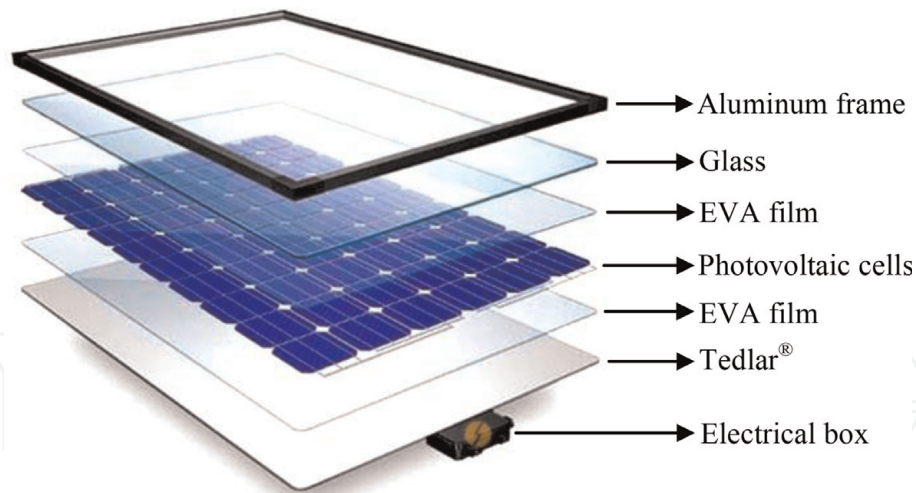


**Figure 4.**  
 Layers of a photovoltaic module.

Type of PV installation	Ross coefficient
Integrated into the roof	0.058
Small distance to the roof (<10 cm)	0.036
Great distance to the roof (>10 cm)	0.027
Free	0.020

**Table 2.**  
 Ross coefficients,  $K_S$ .

Description	Values
Layer thickness of EVA, $d_{EVA}$	0.5 mm
Layer thickness of Glass, $d_{Glass}$	0.4 mm
Layer thickness of Tedlar®, $d_{Tedlar}$	0.15 mm
Thermal conductivity of EVA, $k_{EVA}$	0.34 W/m <sup>2</sup> K
Thermal conductivity of Glass, $k_{Glass}$	1.0 W/m <sup>2</sup> K
Thermal conductivity of Tedlar®, $k_{Tedlar}$	0.167 W/m <sup>2</sup> K

**Table 3.**  
PV layer thicknesses and thermal conductivity of some elements [6].

where:

$d_{Glass}$  is the thickness of the glass.

$d_{EVA}$  is the thickness of the ethylene vinyl acetate (EVA).

$d_{Tedlar}$  is the thickness of the Tedlar®

$k_{Glass}$  is the thermal conductivity of the glass.

$k_{EVA}$  is the thermal conductivity of the ethylene vinyl acetate (EVA).

$k_{Tedlar}$  is the thermal conductivity of the Tedlar®.

By knowing the approximate temperature of the photovoltaic cell and isolating the term Tedlar® in Eq. (24), the temperature at the lower surface of the Tedlar® layer is estimated by Eq. (26) [13]:

$$T_{Tedlar} = T_{Cell} - \left[ \frac{\dot{Q}}{\frac{d_{Glass}}{k_{Glass}} + \frac{d_{EVA}}{k_{EVA}} + \frac{d_{Tedlar}}{k_{Tedlar}}} \right] \quad (26)$$

## 7. Temperature of the absorption plate and its occupation in the thermoelectric area

Much of the radiation on photovoltaic panels is absorbed as heat flowing through the constituent layers. To calculate the temperature of the absorption plate, the parameters shown in **Table 4** take into account the dimensions of the photovoltaic plate. The internal temperature of the plate is determined by Eq. (27) [13, 14].

The temperature on the hot side of the thermoelectric module is considered to be the internal temperature of the absorption plate given by Eq. (28):

$$T_{int,board} = T_{Tedlar} - \frac{L_A}{\kappa_A A_A} \quad (27)$$

where:

$L_A$  is the thickness of the absorption plate.

$k_A$  is the thermal conductivity of the absorption plate.

Definition	Values
Thickness, $L_A$	0.005 m
Thermal conductivity, $k_A$	237 W/m <sup>2</sup> °C <sup>-1</sup>
Absorption plate area, $A_A$	0.0643 m <sup>2</sup>

**Table 4.**  
Characteristics of the absorption plate.

$A_A$  is the area of the plate that absorbs heat.

$T_{Tedlar}$  is the temperature of Tedlar®.

$T_{int,board}$  is the internal temperature of the absorption plate.

The area occupied by thermoelectric modules is a limiting factor for determining the size of the thermoelectric conversion. To estimate the area that the thermoelectric system will occupy, one can use Eq. (28):

$$A_T = w \ell N_T \quad (28)$$

where:

$A_T$  is the total area of the TEG module.

$w$  is the width of the TEG.

$\ell$  is the length of the TEG.

## 8. Determination of the power obtained from a TEG

The power generated by a TEG depends on the internal temperature in the thermoelectric absorption plate, which is an essential parameter for determining the thermoelectric energy generated. Therefore, using Eq. (18) for the considered parameters, the load current can be expressed by Eq. (29):

$$I_{R_L} = \frac{N_s \alpha (T_{int,board} - T_{amb})}{\frac{N_s R_i}{N_p} + R_L} \quad (29)$$

Reordering Eq. (19) for the data parameters, the load voltage is finally determined by Eq. (30):

$$V_c = R_L \left[ \frac{N_s \alpha (T_{int,board} - T_{amb})}{\frac{N_s R_i}{N_p} + R_L} \right] \quad (30)$$

The maximum power of the thermoelectric generation given by Eq. (31) occurs when the internal resistance  $R_i$  is equal to the load resistance  $R_L$ :

$$P_{L,max} = \frac{N_T [\alpha (T_{int,board} - T_{amb})]^2}{4 R_L} \quad (31)$$

## 9. Case study

In this case study, the steps used in the laboratory of CEESP-UFSM to determine the production capacity of a small photovoltaic-thermoelectric cogeneration assembly are shown. The temperature estimation used as input parameter the data of the automatic meteorological station of the National Institute of Meteorology (INMET) for the city of Santa Maria-RS, Brazil, in the period of January 17, 2018–January 23, 2018. The same methodological procedure of this case study can be used to any other location by taking into account the historical temperature data of the place.

In the simulations performed for this section, the reference photovoltaic module is the YL010P-17B 1/13 from the manufacturer YINGLI SOLAR with the characteristics described in **Table 5**. As a prototype, the parameters of this TEG module using the bismuth telluride thermoelectric element are listed in **Table 6**. From the data of solar radiation, ambient temperature and wind speed, it was possible to estimate

Description	Values
Rated voltage	17.1 V
Rated current	0.59 A
Open circuit voltage	24.8 V
Short circuit current	0.65 A
Peak power	$10 \pm 5\% W_p$
Conversion efficiency	11.1%
External module area	$0.09 \text{ m}^2$

**Table 5.**  
Data of the photovoltaic modules, YL010P-17B 1/13.

Description	Values
Maximum voltage	15.4 V
Maximum current	10.5 A
Internal resistance	$1.24 \Omega$
Maximum temperature variation	$67^\circ\text{C}$
Seebeck coefficient	$0.02875 \text{ V/K}$
Thermoelectric junctions	127 pairs
Width, $w$	40 mm
Length, $\ell$	40 mm
Thickness	3.9 mm

**Table 6.**  
Parameters of the thermoelectric module.

with Eq. (23) the temperature of the photovoltaic cell. The temperature of the Tedlar® layer is given by Eq. (26) with the thermal flow directed to the thermoelectric generator. With this, the load power generated by the thermoelectric modules is determined with Eq. (31) with the modules subjected to a positive temperature gradient, i.e. the temperature of the Tedlar® layer is higher than the ambient temperature.

The thermoelectric microgenerator used in this case study is composed of three parts, absorption plate, thermoelectric modules and heat sink, as shown in **Figure 5** considering the dimensions and the internal temperature of the photovoltaic plate. A thin layer of thermal paste was used to improve the heat transfer between the photovoltaic module and the constituent layers of the thermoelectric microgenerator. The electrical connections of the thermoelectric microgenerator are shown in **Figure 6** where the thermoelectric modules are arranged in series in a total of six modules which in turn are connected in parallel with the photovoltaic module.

**Figure 7** is the record of temperatures measured in the week between January 17, 2018, and January 23, 2018. The blue line data represents the temperature of the photovoltaic cell, and the red line represents the ambient temperature. Notice that there is a significant difference between the ambient temperature and the temperature of the photovoltaic cell. With this, heat reduces the efficiency of the photovoltaic cells but has a reasonable potential for thermoelectric cogeneration. The internal temperature of the absorption plate is the same as the hot surface of the

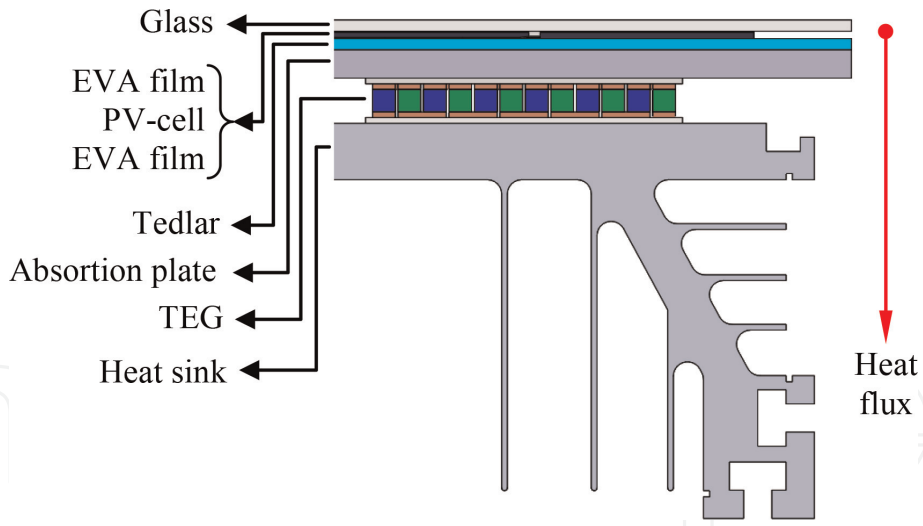


**Figure 5.**  
 Layer distribution of the PV-TEG system.

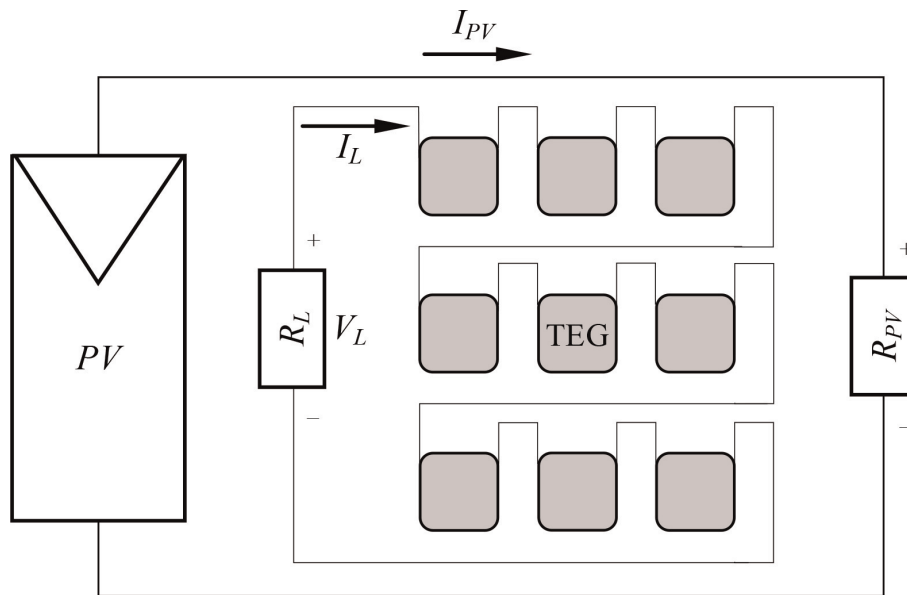


**Figure 6.**  
 General diagram of PV-TEG cogeneration.

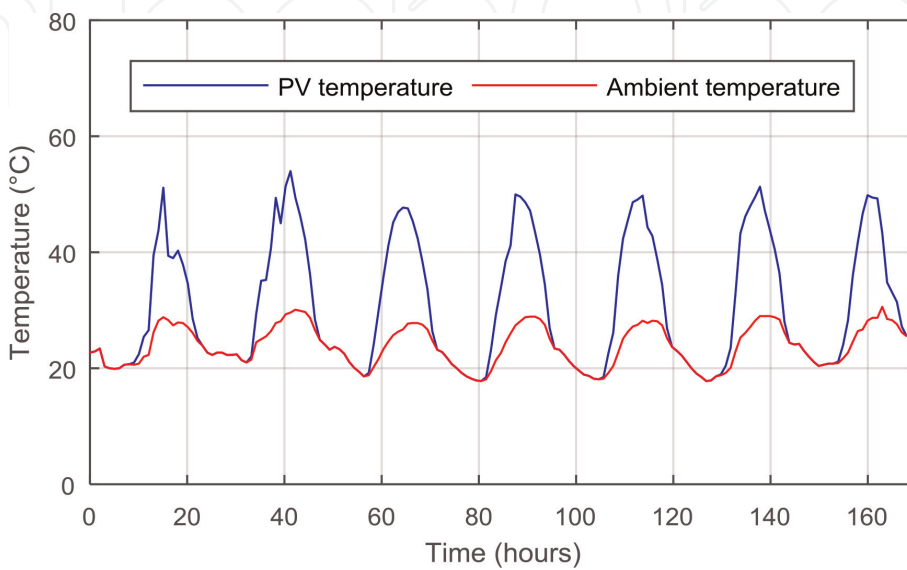


**Figure 7.**  
 Temperatures of the photovoltaic cell and the environment.



thermoelectric modules and is calculated by Eq. (27). The average temperature estimated for the absorber plate is  $0.0002^{\circ}\text{C}$  which is lower than the temperature of the Tedlar® layer given by Eq. (26).

The area of the heat-absorbing plate corresponds to 71.44% of the area of the photovoltaic panel, which is  $0.09\text{ m}^2$ . **Figure 8** shows the temperature variation in the photovoltaic cell, the temperature of the absorber plate and the ambient temperature. In this figure, the theoretical temperature of the absorber plate is slightly less than the temperature of the photovoltaic cell and is also significantly higher than the ambient temperature. The greater is the difference between these parameters, the greater is the thermoelectric generation as specified by Eq. (31). The most important parameter for increasing thermoelectric generation is the temperature difference between the hot side and the cold side of the module. The average temperature difference between the TEG surfaces in the practical tests was  $23.88^{\circ}\text{C}$  for the given period. This estimation considered that the heat sink temperature was maintained at  $5^{\circ}\text{C}$  above room temperature.

**Figure 9** is an estimate of the thermoelectric generation calculated for the period from January 17, 2018, to January 23, 2018.

The total thermoelectric generation estimated with the data used in this section is  $96.86\text{ W}$  for a 1-week period accounting for 71 hours of electricity generation. The temperature variation between the absorber plate and the TEG ambient temperature was always positive. During this period, the estimated average of hourly energy production in the TEG microgenerator was  $1.37\text{ Wh}$ .

**Figure 10** shows the theoretical electricity either in the photovoltaic module or in the TEG module during the period considered in this section. Soon after, the power of the thermoelectric generator was estimated using Eqs. (23)–(31). The total theoretical energy generated in the photovoltaic module was  $479\text{ W}$ , and the total energy generated in the TEG module was  $96.86\text{ W}$ .

It is important to mention at this point that both generation profiles shown in **Figure 10** have the same shape a part of their scales. This is due to the fact that there is a proportional correlation between incident solar irradiance and the bottom surface of the photovoltaic module where the TEGs are connected to the absorber plate.

**Table 7** shows the theoretical electricity generated by the cogeneration system described in this case study. This shows that after coupling the TEG module to the photovoltaic panel, the total electric energy generated had an increase of 20.2% when compared to the photovoltaic system without cogeneration.

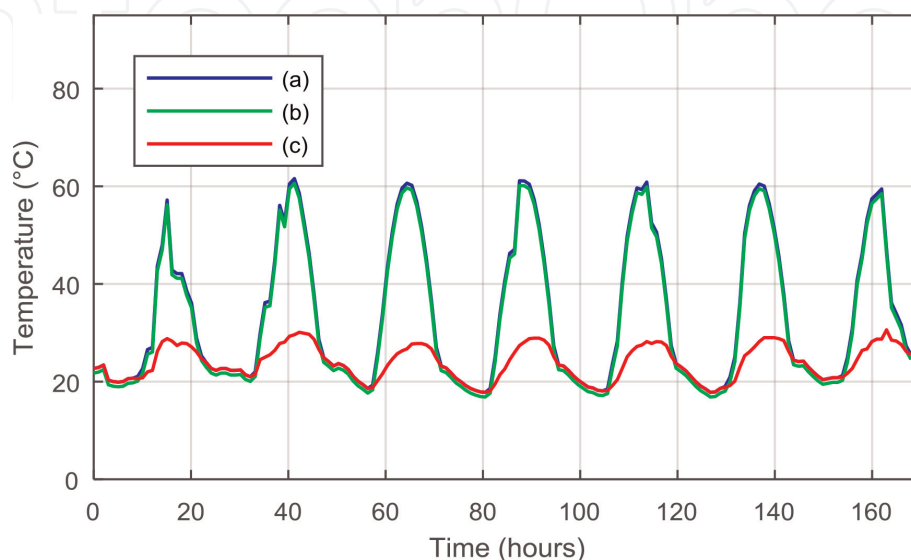


**Figure 8.** Temperatures of (a) PV-cell, (b) inner face of the absorption plate, and (c) ambient.

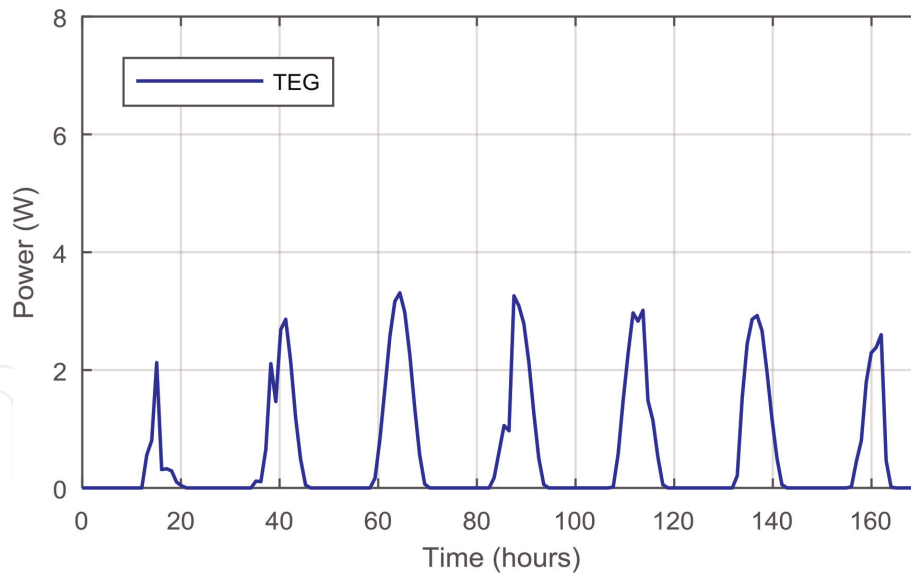


**Figure 9.**  
 Estimation of the TEG energy.

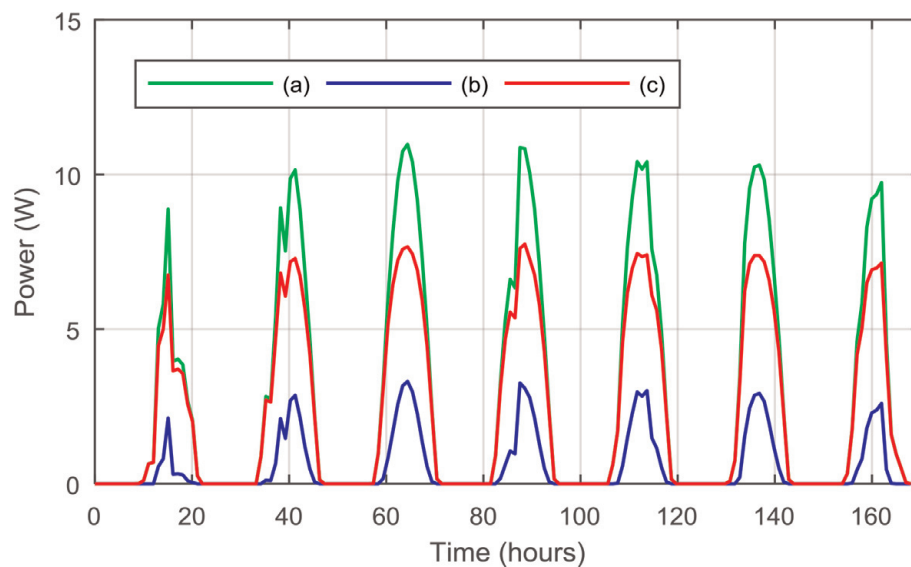


**Figure 10.**  
 Energy generation profiles: (a) PV module with cogeneration, (b) TEG module, and (c) PV module without cogeneration.

Electric power	
PV module without cogeneration	388.14 W
PV module with cogeneration	479 W
TEG module	96.86 W
PV + TEG cogeneration	575.86 W

**Table 7.**  
 Total theoretical electric power along a week.

## 10. Conclusion

This chapter analyses the use of thermoelectric generators in photovoltaic cogeneration to exploit the residual thermal energy in a direct, renewable, viable,

efficient and sustainable way. It shows that the capture of the residual energy by the Seebeck effect for cogeneration of electric energy can be useful and efficient in several fields of human activities concerning its easy application, low weight, reduced size and simplicity of operation.

A thermoelectric generator operates noninvasively, indirectly taking advantage of the thermal energy of other systems where it is inserted without negative interference in the process. Another characteristic of the thermoelectric generators is their modularity, which allows the expansion of cogeneration to match certain output power or to change their way in association with other thermoelectric modules.

Even if the thermoelectric generation is still limited to low temperature gradients ( $\Delta T < 25^\circ\text{C}$ ), it can be seen that this technology will have benefits when associated with photovoltaic systems. This is due to the increase of the heat transfer from photovoltaic modules to the environment, at the same time, generating an additional amount of electric energy in the TEG module without increasing any further conversion area exposed to the sun.

The heat transfer technique used in the case study described in this chapter shows that it is possible to exploit the residual thermal energy of a photovoltaic module to improve its own performance. This has been suggested as a practical way to improve thermoelectric cogeneration (Seebeck effect) with photovoltaic modules (PV-TEG) and to increase energy efficiency of other associated hybrid systems.

The possibilities of thermoelectric-photovoltaic cogeneration are still greatly reduced by the limitations imposed by their low temperature gradients and efficiency. An improvement can be expected, for example, with a significant increase in the number of interconnected thermoelectric modules. Another point is that there is a limitation in the contact area between the thermocouples and the bottom surface of the photovoltaic module. Of course, this would increase the assembly cost and complexity of the generator, which could only be justified in particular cases that would not allow any other alternatives.

IntechOpen


### **Author details**

Felix A. Farret\* and Emanuel A. Vieira

Center of Excellence in Energy and Power Systems (CEESP), Federal University of Santa Maria (UFSM), Santa Maria, Brazil

\*Address all correspondence to: [fafarret@gmail.com](mailto:fafarret@gmail.com)

### **IntechOpen**

© 2020 The Author(s). Licensee IntechOpen. Distributed under the terms of the Creative Commons Attribution - NonCommercial 4.0 License (<https://creativecommons.org/licenses/by-nc/4.0/>), which permits use, distribution and reproduction for non-commercial purposes, provided the original is properly cited. 

## References

- [1] Vieira E. Increasing the Efficiency of Photovoltaic Modules with Utilization of Thermal Energy for Thermoelectric Generation of Solid State [master thesis]. Santa Maria, RS: Post-Graduation Program in Electrical Engineering; 2018. p. 128
- [2] Farret FA, Simões GM. Integration of Renewable Sources of Energy. 2nd ed. Hoboken, New Jersey, USA: John Wiley and Sons Ltd; 2018. LCCN: 2017007716
- [3] Radhakrishnan R. "A Review of Thermoelectric, Handbook Macro to Nano," D.M. Rowe (editor). Materials and Manufacturing Processes. 2008; **23**(6):626-627. DOI: 101080/10426910802135819
- [4] Ismail B, Ahmed W. Thermoelectric power generation using waste-heat energy as an alternative green technology. Recent Patents on Electrical Engineering. 2009; **2**(1):27-39
- [5] Riffat SB, Ma X. Thermoelectrics: A review of present and potential applications. Applied Thermal Engineering. 2003; **23**(8):913-935. DOI: 101016/s1359-4311(03)00012-7
- [6] Daud MMM, Nor NBM, Ibrahim T. Novel hybrid photovoltaic and thermoelectric panel. In: 2012 IEEE International Power Engineering and Optimization Conference, PEOCO 2012: Conference Proceedings; 2012. pp. 269-274
- [7] Hsiao YY, Chang WC, Chen SL. A mathematic model of thermoelectric module with applications on waste heat recovery from automobile engine. Energy. 2010; **35**(3):1447-1454. DOI: 10.1016/j.energy.2009.11.030
- [8] Carvalho C.A.R. of Feasibility Study of the Use of Heat Exhaust for Generation of Electric Energy in Automobiles [master thesis]. Taubaté University; 2012. p. 68
- [9] Phillips SS. Characterizing the thermal efficiency of thermoelectric modules. Bachelor of Science, Massachusetts Institute of Technology. Massachusetts: Cambridge; 2009:1-9
- [10] Yodovard P, Khedari J, Hirunlabh J. The potential of waste heat thermoelectric power generation from diesel cycle and gas turbine cogeneration plants. Energy Sources. 2001; **23**(3):213-224. DOI: 101080/00908310151133889
- [11] Ross RGJ. Interface design considerations for terrestrial solar cell modules. In: Photovoltaic Specialist Conference 1976; 1976. pp. 801-806
- [12] Ross RGJ. Flat-plate photovoltaic array interface design optimization. In: Proc. 14th IEEE Photovoltaic Specialist Conference 1980; 1980. pp. 1126-1132
- [13] Krauter S, Preiss A. Comparison of module temperature measurement methods. In: Conference Record of the IEEE Photovoltaic Specialists; 26617(4): 2009. pp. 333-338. DOI: 10.1109/pvsc.2009.5411669
- [14] Inropera FP, DeWitt DP, Bergman TL, Lavine AS. Fundamentals of heat and mass transfer. In: Water. Vol. 6th. 2002. p. 997. ISBN: 9780471457282